Lin et al. Sustainable Environment Research (2019) 29:22
https://doi.org/10.1186/s42834-019-0021-8

Sustainable Environment Research

TECHNICAL NOTE Open Access

Deciphering the effect of citric acid on arsenic adsorption with phosphorene in aqueous solution

Yu-Jung Lin[1], Wen-Zhi Cao[2], Tong Ou Yang[2], Chun-Hua Feng[1] and Chang-Tang Chang[3*]

Abstract

This paper presents the first attempt to explore the potential of phosphorene as an adsorbent for arsenic [AS(III) and As(V)] removal under competition adsorption with citric acid (CA). In this study, the phosphorene was prepared by the exfoliation method. Results showed that CA reduced As(III) adsorption due to the lower stability constant of organic-As(III) complexes. The adsorption capacity with phosphorene was enhanced with a decrease in the initial concentration of CA. The adsorption rates for As(III) and As(V) were 0.033 and 0.069 min^{-1}, respectively, according to kinetics analysis. The maximum adsorption capacity obtained using the Langmuir model was 8.9 mg g^{-1} for As(III) at pH 7 with 0.1 mM CA addition, and the As(V) adsorption capacity of phosphorene was 20 mg g^{-1}.

Keywords: Phosphorene, Competition adsorption, Citric acid, Arsenic

Introduction

Even at a low exposure dosage, arsenic remains the most toxic element to humans [1]. It shows multiple and complex forms. Dissolved states of arsenic exist with methylation of arsenic compounds or inorganic arsenate and arsenite. Moreover, the speciation varies, depending on the pH and oxidation-reduction environment [2] as shown in Fig. 1. $H_2AsO_4^-$ is dominant at low pH (less than pH 6.9), while $HAsO_4^{2-}$ becomes dominant at higher pH ($H_3AsO_4^0$ and AsO_4^{3-} may be present in extremely acidic and alkaline conditions respectively). As(III) is 60 times more toxic than As(V).

Various adsorbents have been developed and applied from different cost-effective sources [3]. The low-cost material graphite has been intensively investigated as an adsorbent for various heavy metal emoval [4–6]. Similar to graphene, phosphorene has a puckered hexagonal atom structure. Phosphorene, the youngest member (according to the chronology of its discovery) of the exotic class of two-dimensional crystals is attracting considerable attention because of its desirable features and finite band gap. First, it possesses a high carrier mobility of ~1000 $cm^2 V^{-1} s^{-1}$ for hole transport [7–11]. Second, it presents a high dispersion capability of the isotropic band in the Brillouin zone close to the Fermi level [8].

Citric acid (CA) is one of the organic ligands commonly present in natural water systems. The speciation of metals in solution may enhance adsorption if the ligands themselves are adsorbed onto the mineral surface [12]. According to some research, adsorption is an efficient method for some specified solutes under lower concentrations, especially for the heavy metals in wastewater.

In this study, phosphorene was used for arsenic adsorption in an aqueous solution, and the effects of CA addition were discussed. The temperature, initial concentration, pH, and concentration of CA were controlled to determine the maximum efficiencies of arsenic removal under different conditions.

Materials and methods

Phosphorene catalysts were prepared by the exfoliation method [13]. First, 75 mg of black phosphorous (99.995%, Aldrich) and 10 mL of *N*-methyl-2-pyrrolidone (99% C_5H_9NO, Alfa Aesar, UK) were ultrasonicated in bottles for 8 h. The liquid (a mixture containing N-methyl-2-pyrrolidone and black phosphorous) was purged with N_2 after being ultrasonicated for 40 min for black phosphorous to be exfoliated effectively and

* Correspondence: ctchang@niu.edu.tw
[3]Department of Environmental Engineering, National Ilan University, Ilan 26047, Taiwan
Full list of author information is available at the end of the article

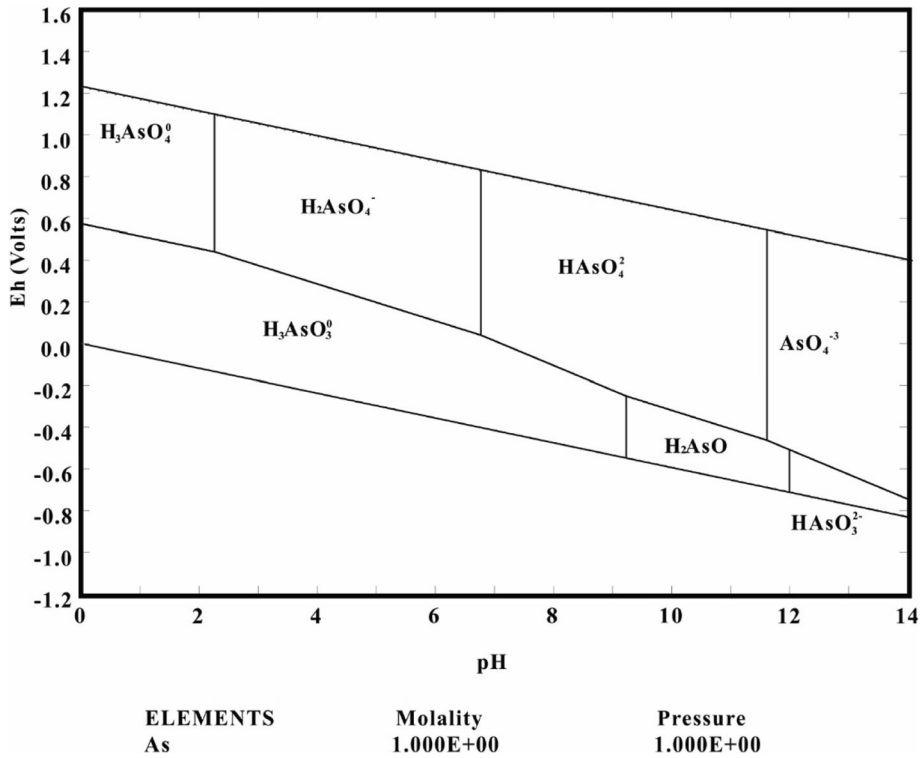

Fig. 1 Eh-pH diagram for aqueous As species in the system As-O_2-H_2O at 25 °C and 0.1 MPa total pressure

uniformly. Subsequently, the liquid was centrifuged at 3000 rpm for 10 min. Arsenic [As(III)] solutions were prepared by adding As_2O_3 (High-Purity Standards, USA) stock solutions. As(V) was prepared from stock solution of $Na_2HAsO_4{\cdot}7H_2O$ (Merck standard solutions, USA). For the batch method, 40 μL of the adsorbent (phosphorene) was added to a capped glass vial containing 250 mL of arsenic solution at pH = 7. The pH value was maintained at pH 7 by using NaOH and HCl. Exactly 2 mL of the solution was extracted and placed in a test tube to determine the initial concentration. The contact times (from 1 to 25 min) were used. Table 1 lists the experiment parameters. The concentration of the extracted solution was analyzed with an inductively coupled plasma-atomic emission spectroscopy system (Agilent, G8000A).

Table 1 Experiment parameter

Experiment parameter	Operation parameter
Temperature (°C)	15, 25, 35, 45
Concentration of As (mg L^{-1})	0.5, 1.0, 2.0, 4.0
pH	3, 5, 7, 9
Adsorbent dosage (g L^{-1})	0.1, 0.2, 0.5, 0.8
As species	As(III), As(V)
Concentration of CA (mM)	0.1, 1.0

The surface morphology of the phosphorene adsorbent was observed using an atomic force microscope (AFM, North Atlantic Oscillation-NAO, NC, USA). A sample of phosphorene was used to conduct zeta potential measurements with a zeta potential instrument (Nano ZS90, Malvern, UK). The samples of the phosphorene adsorbent before and after As(III) sorption of the spectra were recorded on a Fourier-transform infrared spectroscopy (FTIR) spectrophotometer (Spectrum 100, Perkin Elmer, USA) in the wavenumber range of 600–4000 cm^{-1}.

Results and discussion

Characteristics

Figure 2a shows the AFM image of a 5.58 nm-thick flake with a phosphorene capping layer on top. This flake is 1.9 nm thicker than that reported by Das et al. [12]. Figure 2b presents the AFM images of exfoliated multilayer phosphorene sheets made from black phosphorus coated on glass substrates. The images prove the presence of various shapes and sizes of phosphorene sheets. The thickness of the phosphorene in Fig. 2c is approximately 5.58 nm. The profile of the phosphorene nanosheets exhibits clear edges and a thickness range of ca. 4.6–6.0 nm. The AFM results indicate that the large nanofilms mainly contain three to five layers of phosphorene. The AFM characterization clearly shows that with an exfoliation time 48 h, the large flakes break down mainly into

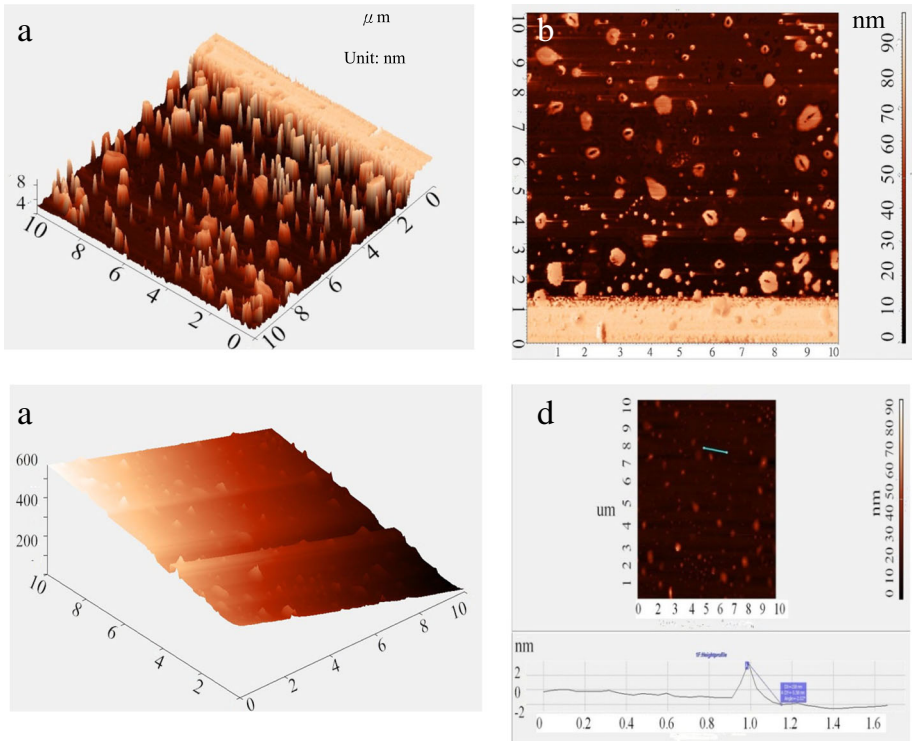

Fig. 2 AFM images of phosphorene (**a**) 3D view of phosphorene, (**b**) exfoliated multilayer of phosphorene sheets, (**c**) 3D view of phosphorene, (**d**) fix site measurement

monolayer and bilayer phosphorene [14]. The surface charge density increased with pH. The surface charge is negatively charged under $pH > pH_{zpc}$ (point of zero charge) thus showing a higher affinity for cations. The surface charge is positive under $pH < pH_{zpc}$, and has a higher affinity for anion.

The ZPC of phosphorene under a hydration state is 3.0. Therefore, we find a positive charge when the pH is below 3.0, as shown in Fig. 3a. The vibration peak of As-O shifted from 948 to 965 cm^{-1}, and the function groups located at 1591 cm^{-1} represent the asymmetry vibration peak of $-COO^-$ [15], as shown in Fig. 3b. This means the blue shift was caused by the vibration peak of As-O after 10 mg L^{-1} of As(III) adsorption (red curve). This illustrates that the surrounding As-O in the chemical environment varied during As(III) adsorption when using phosphorene.

From Fig. 3c, the POx peak is at 130 eV and the P-C bond is located at 131.5 eV and the content of P-C is calculated to be 45.1% by XPS-fit software. Furthermore, the P-O bond was located at 129.7 eV and the content of P-O was 54.9%, which is higher than that of the P-C bond. This benefits As(III) adsorption since As-O can coordinate with P-O, making As(III) adsorption easier [16].

Performance assessment

Comparisons of phosphorene adsorption with various adsorbents are presented in Table 2. Under similar conditions, phosphorene has the greatest adsorption capacities.

Effect of concentration

For the assessment of the effect of the concentration on the arsenic adsorption capacity, the concentrations of As(III) in the solutions were controlled at 0.5, 1.0, 2.0 and 4.0 mg L^{-1}. The contact times ranged from 1 to 25 min. The dosage of the adsorbent, pH and temperature were controlled under 0.1 ± 0.01 g L^{-1}, 3.0 to 9.0 and 25 ± 0.5 °C, respectively. The adsorption capacity of arsenic onto graphene oxide/$CuFe_2O_4$ was 5, 13.6, 22.3 and 26.5 mg g^{-1} at concentrations of 0.5, 1.0, 2.0 and 4.0 mg L^{-1}, respectively [19]. As the concentration of arsenic was increased, the adsorption capacity increased (Fig. 4a). However, the adsorption capacities decreased to 2.4, 4.4, 6.9 and 8.0 mg g^{-1} after 0.1 mM of CA was added. The reduced adsorption is probably due to the fact that the CA is an organic acid with oxygen containing functional groups. It formed binding bridge with adsorption sites at lower concentration. The complex cation ions were adhered to a surface of the adsorbent. Besides, CA can adversely affect adsorption with cation ions due to precipitate formation by complexing actions when the concentration of CA is higher [20].

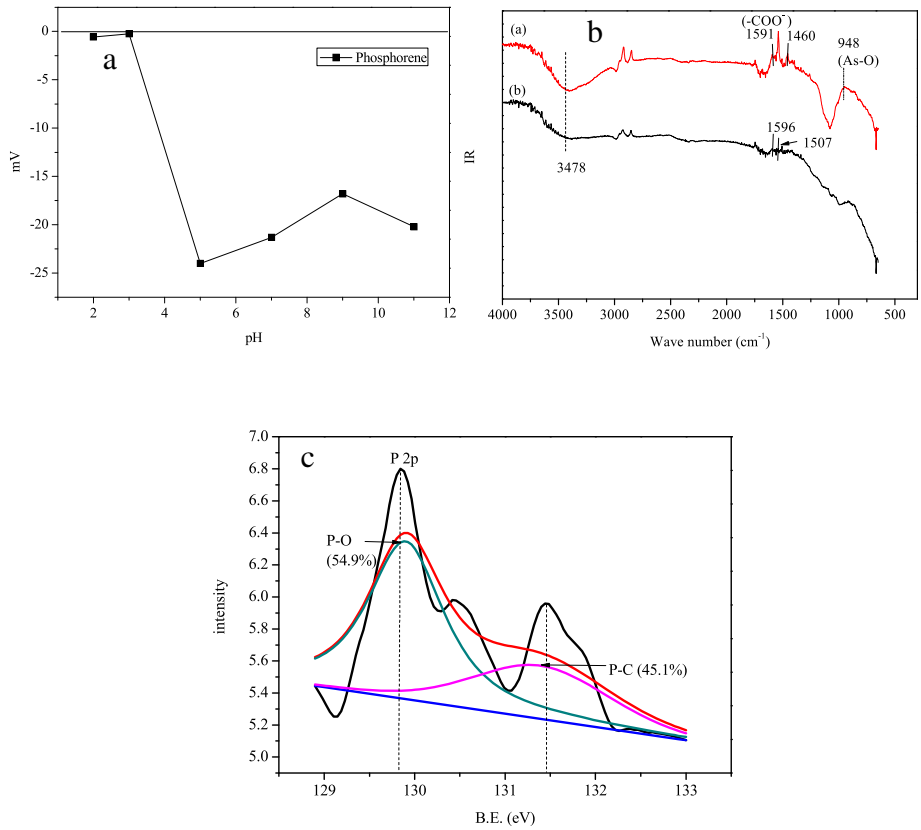

Fig. 3 Phosphorene characterization (**a**) zeta potential of phosphorene and graphene oxide, (**b**) FTIR of phosphorene (black curve: before As(III) adsorption, red curve: a fter As(III) adsorption), (**c**) P2p of phosphorene with XPS

Effect of temperature

The temperatures were controlled at 15, 25, 35, and 45 °C to understand the effect of temperature on arsenic adsorption capacity. When the CA was added to the arsenic solution, the efficiencies of arsenic adsorption were 18, 39, 59, and 60% at 15, 25, 35, and 45 °C, respectively (Fig. 4b). The adsorption capacities of arsenic onto phosphorene were 2.1, 4.4 5.8 and 8.0 mg g^{-1} at 15, 25, 35, and 45 °C, respectively. Adsorption arises from electrostatic interaction, which is usually associated with low adsorption heat.

Effect of CA concentration

In this study, the concentration of arsenic was fixed at 1 mg L^{-1} for arsenic adsorption with phosphorene as the adsorbent. The adsorption capacities of As(III) were calculated as 4.4 and 2.1 mg g^{-1} in the presence of 0.1 and 1 mM of CA, respectively. The results obtained with phosphorene as the adsorbent exhibited similar trends compared with the adsorbents of graphene. The efficiency of arsenic adsorption with the addition of 0.1 mM CA was only 40%. In contrast, it was 12% with the addition of 1 mM CA (Fig. 4c). Hence, we can conclude that the arsenic adsorption capacity decreases dramatically as the concentration of CA increases.

Effect of pH

The pH levels of the arsenic solutions were set to 3, 5, 7 and 9 to determine the effect of pH on arsenic removal efficiency. The efficiencies of arsenic adsorption were 80, 50, 40 and 22% at pH 3, 5, 7 and 9, respectively, at 25 °C

Table 2 Comparisons of phosphorene adsorption with various adsorbents

Graphene species	Particle size (nm)	pH_{zpc}	As species	Adsorption capacities (mg g^{-1})	Reference
Fe_3O_4-graphene	–	–	As(III)	0.0103	[17]
Fe_3O_4-graphene-MnO_2 composites	10	7	As(V)	12.2	[18]
GO-ZrO $(OH)_2$	3.27	7	As(III)	17.2	[3]
phosphorene	5.58	3.0	As(III)	20	This study

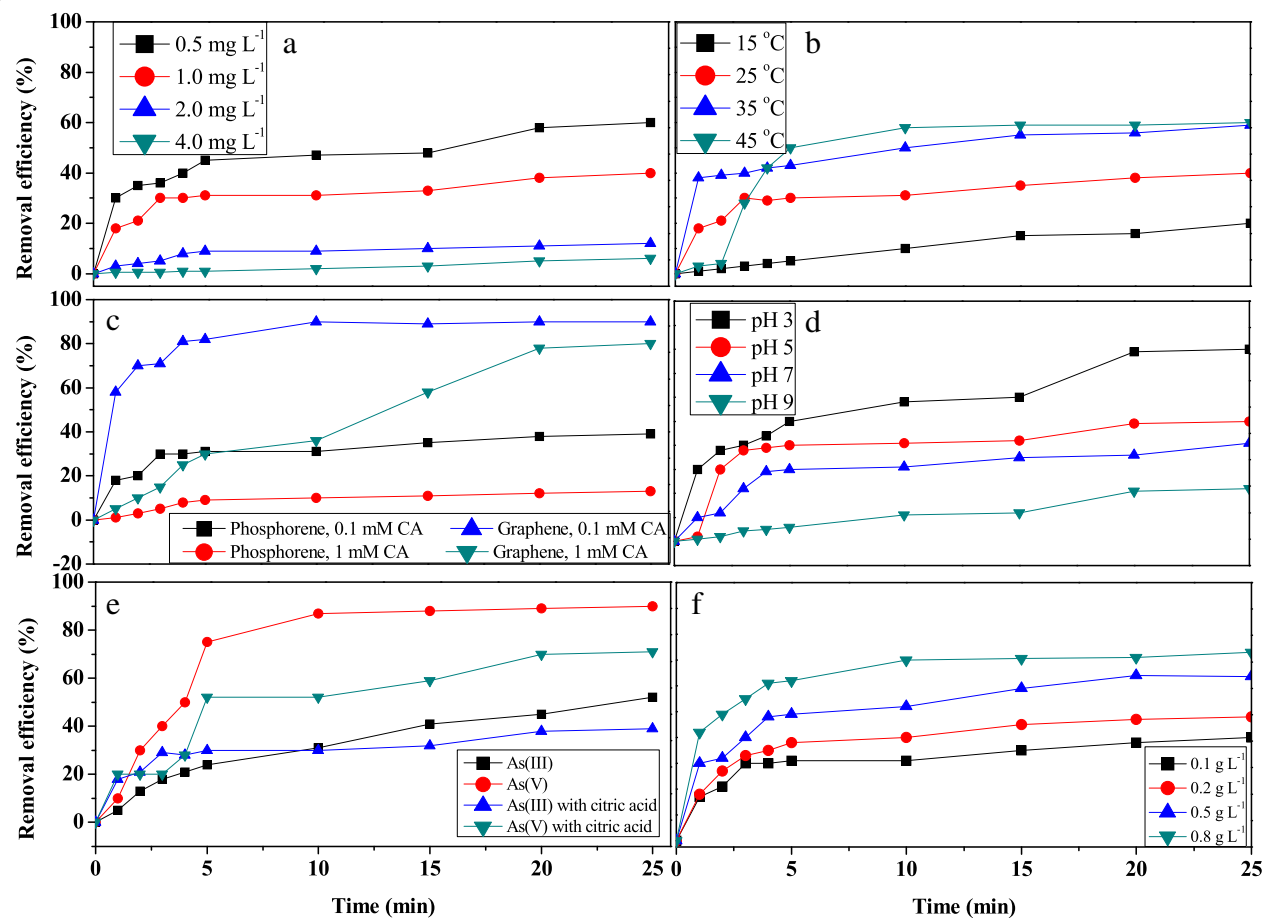

Fig. 4 Effects of environmental parameters on performance (**a**) Concentration, (**b**) Temperature, (**c**) CA concentration, (**d**) pH, (e) Valance, (**f**) Dosage. Conditions: initial As(III) or As(V) concentration = 1.0 mg L^{-1}; solution temperature = 25 °C; pH = 7.0; concentration of CA = 0.1 mM

with phosphorene dosages of 0.1 g L^{-1}, 0.1 mM of CA in 1 mg L^{-1} arsenic solution, as shown in Fig. 4d.

At pH levels above 7, the anionic species ($HAsO_4^{2-}$) began to form. The removal efficiencies were 80, 70, 50 and 28% at pH 3, 5, 7 and 9, respectively, without the addition of CA [21]. The adsorption efficiency slightly decreased with CA addition. Oxygen is believed to be a function of the phosphorene surface. As a result, the mechanism of adsorption is affected and, consequently, the affinity of CA for the phosphorene surface is decreased [22]. The influence of pH on arsenic adsorption revealed in this study is in agreement with the results reported by previous researchers [23, 24].

Effect of as valance

The assessment of phosphorene for its adsorptive properties was carried out by understanding the valance effect of arsenic species, including As(III) and As(V). The adsorption efficiencies for As(III) and As(V) were calculated to be 53 and 90%, respectively, at 25 °C, pH 7, and phosphorene dosage of 0.1 g L^{-1}, with the concentration the arsenic solution being 1 mg L^{-1}. However, the adsorption efficiencies for As(III) and As(V) decreased to 40 and 72%, respectively, with the addition of 0.1 mM of CA, as shown in Fig. 4e. Grafe et al. [22] used iron ore for As(III) adsorption competing with CA and the adsorption capacity was also decreased after adding CA, since surface affinity for As(III) was decreased when adding CA at lower pHs.

Effect of dosage

The dosages of the phosphorene were varied from 0.1 to 0.8 g L^{-1} to determine the arsenic removal efficiency. The adsorption efficiency was 73% at pH 7, 25 °C and 0.1 mM of CA with 0.8 g L^{-1} of phosphorene in 1 mg L^{-1} arsenic solution (Fig. 4f). The adsorption efficiency decreased with the increase of CA concentration. For comparison, the adsorption efficiency reached 80% without CA addition [21].

Adsorption isotherm analysis

The Langmuir, Freundlich, Temkin and Harkins-Jura models were used to understand the behavior of As(III)

Table 3 The constant of isotherms

	Langmuir	Freundlich	Temkin	Harkins-Jura
a (L mg^{-1})	0.229			
q (mg g^{-1})	20			
n		1.13		
K (mg g^{-1})		1.49		
K_T (J g^{-1})			22.3	
B (J mol^{-1})			0.046	
A_H (g L^{-1})				57.1
B_H (mg^2 mol^{-1})				−21.8
R^2	0.951	0.947	0.788	0.941

adsorption in phosphorene. The results are shown in Fig. 5 and Table 3. From Table 3, the fitting correlation coefficient of the Freundlich model is 0.947 and the constant n is greater than 1, indicating a favorable adsorption reaction. The correlation coefficient of linear regression analysis of the Langmuir model is 0.951, and the maximum adsorption capacity of phosphorene is calculated as 20 mg g^{-1}. Therefore, the Langmuir model is proven to be more suitable for describing the adsorption behavior with phosphorene. The correlation coefficients of As(III) adsorption with phosphorene using the Temkin and Harkins-Jura models were found to be 0.788 and 0.941, respectively, according to the regression analysis. This indicates that the Temkin model is not suitable for fitting the behavior of As(III) adsorption with phosphorene. However, the Harkins-Jura model is suitable for fitting the behavior of As(III) adsorption with phosphorene. The correlation coefficient of the Temkin model is smaller than that of the Langmuir and Freundlich models, and is also lower than 0.95.

Dynamic analysis

This study investigated the kinetics model of As(III) adsorption with phosphorene under different temperature conditions. The results are shown in Table 4. The correlation coefficient of pseudo second order kinetics fitting is slightly higher than that of the first-order kinetic model. The correlation coefficient is between 0.866 and 0.999, indicating that the pseudo second order kinetics model is more suitable for fitting the experimental data in this study.

The parameters were combined with the relevant diffusion model of the intra particle diffusion analysis result with phosphorene. The correlation coefficient of 0.906 (Table 4) was too small and indicated that the intra particle diffusion model did not show good results. The mass transfer coefficients (K_{id}) are 0.39, 1.8, 5.7 and 0.34 mg g^{-1} $min^{1/2}$ at 15, 25, 35 and 45 °C, respectively, as shown in Table 4. The mass transfer coefficient is greater than 1 at temperatures of 25 and 35 °C.

The fitting parameters of Elovich model are shown in Table 4. The correlation coefficients of the Elovich

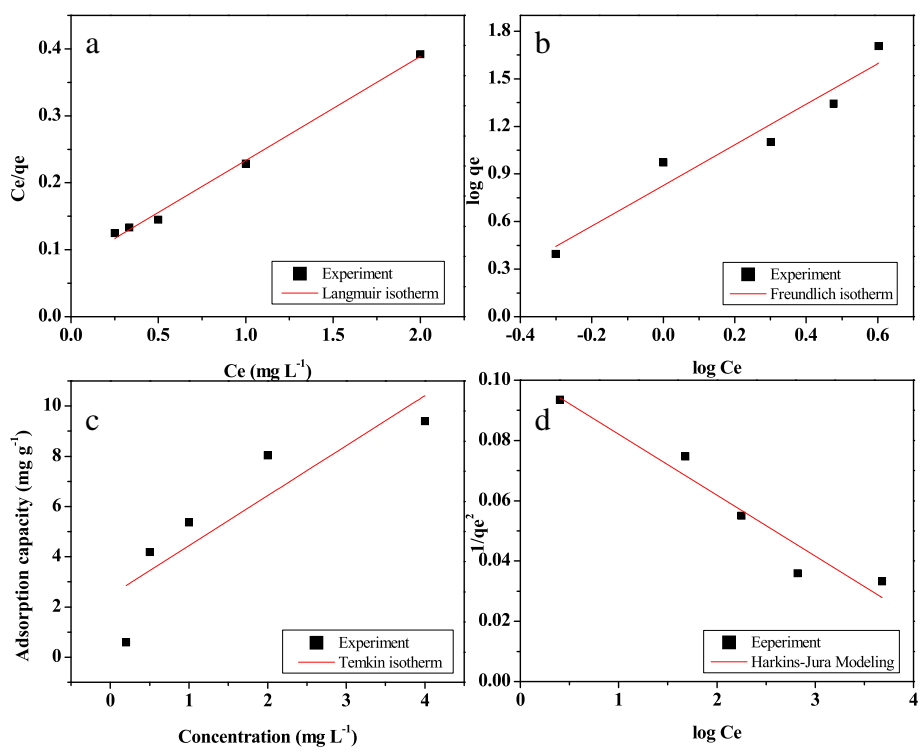

Fig. 5 Isotherms of arsenic adsorption with phosphorene (**a**) Langmuir, (**b**) Freundlich, (**c**) Temkin and (**d**) Harkins-Jura

Table 4 The parameter of kinetic models with the addition of 0.1 mM CA

Pseudo-first-order				
Temperature (°C)	15	25	35	45
k_1 (min^{-1})	0.014	0.024	0.012	0.192
R^2	0.866	0.511	0.977	0.933
Pseudo-second-order				
Temperature (°C)	15	25	35	45
k_2 ($g\ mg^{-1}\ min^{-1}$)	4.0	1.1	0.36	0.15
R^2	0.999	0.999	0.998	0.998
Intra-particle diffusion				
Temperature (°C)	15	25	35	45
I ($mg\ g^{-1}$)	0.038	0.386	0.124	0.579
k_{id} ($mg\ g^{-1}\ min^{1/2}$)	0.39	1.8	5.7	0.34
R^2	0.807	0.906	0.787	0.307
Elovich				
Temperature (°C)	15	25	35	45
a ($mg\ g^{-1}\ min^{-1}$)	0.31	1.37	3.4	8.7
b ($g\ \mu g^{-1}$)	−0.023	−0.023	−0.208	−0.791
R^2	0.887	0.804	0.964	0.919

model are 0.887, 0.804, 0.964 and 0.919, respectively, under the above temperatures. The initial reaction rate ($8.7\ mg\ g^{-1}\ min^{-1}$) is the fastest at 45 °C. As(III) can be diffused more uniformly in the inner pores of phosphorene. The adsorption data fitted well with the Elovich equation, indicating that the adsorption process belongs to heterogeneous diffusion.

Conclusions

The thickness of phosphorene is 5.58 nm, as determined by AFM. The chemical environment of As-O changed during As(III) adsorption with phosphorene, as shown in the FTIR graph. This means the process of adsorption occurred via chemical reactions. The adsorption efficiency decreases slightly when CA mediates the arsenic adsorption at different pH levels. As the concentration of arsenic increases, the adsorption capacity also increases. Furthermore, the arsenic adsorption capacity significantly decreases as the concentration of CA increases.

Acknowledgements
The authors thank Professor Yih-Pey Yang from the Department of Biomechatronic Engineering at National Ilan University for supplying the atomic force microscope. The authors also thank the Ministry of Science and Technology for providing financial support for this project (MOST 105-2622-E-197-010-CC3).

Authors' contributions
YJ carried out the Arsenic adsorption studies, participated in the characterization of materials and drafted the manuscript. WZ carried out novelty development. T participated in the design of the study and performed the statistical analysis. CH participated in its coordination. CT conceived of the study and participated in its design. All authors read and approved the final manuscript.

Competing interests
The authors declare that they have no competing interests.

Publisher's Note
Springer Nature remains neutral with regard to jurisdictional claims in published maps and institutional affiliations.

Author details
[1]School of Environment and Energy, South China University of Technology, Guangzhou 510006, China. [2]College of the Environment and Ecology, Xiamen University, Xiamen 361005, China. [3]Department of Environmental Engineering, National Ilan University, Ilan 26047, Taiwan.

Received: 17 July 2018 Accepted: 10 April 2019
Published online: 07 August 2019

References
1. Mukherjee A, Sengupta MK, Hossain MA, Ahamed S, Das B, Nayak B, et al. Arsenic contamination in groundwater: a global perspective with emphasis on the Asian scenario. J Health Popul Nutr. 2006;24:142–63.
2. Smedley PL, Kinniburgh DG. A review of the source, behaviour and distribution of arsenic in natural waters. Appl Geochem. 2002;17:517–68.
3. Luo XB, Wang CC, Wang LC, Deng F, Luo SL, Tu XM, et al. Nanocomposites of graphene oxide-hydrated zirconium oxide for simultaneous removal of As(III) and As(V) from water. Chem Eng J. 2013;220:98–106
4. Jung C, Heo J, Han J, Her N, Lee SJ, Oh J, et al. Hexavalent chromium removal by various adsorbents: powdered activated carbon, chitosan, and single/multi-walled carbon nanotubes. Sep Purif Technol. 2013;106:63–71.
5. Ge HC, Ma ZW. Microwave preparation of triethylenetetramine modified graphene oxide/chitosan composite for adsorption of Cr(VI). Carbohyd Polym. 2015;131:280–7.
6. Najafabadi HH, Irani M, Rad LR, Haratameh AH, Haririan I. Removal of Cu^{2+}, Pb^{2+} and Cr^{6+} from aqueous solutions using a chitosan/graphene oxide composite nanofibrous adsorbent. RSC Adv. 2015;5:16532–9.
7. Das S, Appenzeller J. Where does the current flow in two-dimensional layered systems? Nano Lett. 2013;13:3396–402.
8. Li LK, Yu YJ, Ye GJ, Ge QQ, Ou XD, Wu H, et al. Black phosphorus field-effect transistors. Nat Nanotechnol. 2014;9:372–7.
9. Liu H, Neal AT, Zhu Z, Luo Z, Xu XF, Tomanek D, et al. Phosphorene: an unexplored 2D semiconductor with a high hole mobility. ACS Nano. 2014;8:4033–41.
10. Das S, Zhang W, Demarteau M, Hoffmann A, Dubey M, Roelofs A. Tunable transport gap in phosphorene. Nano Lett. 2014;14:5733–9.
11. Liu H, Neal AT, Si MW, Du YC, Ye PD. The effect of dielectric capping on few-layer phosphorene transistors: tuning the Schottky barrier heights. IEEE Electr Device L. 2014;35:795–7.
12. Das S, Demarteau M, Roelofs A. Ambipolar phosphorene field effect transistor. ACS Nano. 2014;8:11730–8.
13. Brent JR, Savjani N, Lewis EA, Haigh SJ, Lewis DJ, O'Brien P. Production of few-layer phosphorene by liquid exfoliation of black phosphorus. Chem Commun. 2014;50:13338–41.
14. Bagheri S, Mansouri N, Aghaie E. Phosphorene: a new competitor for graphene. Int J Hydrogen Energ. 2016;41:4085–95.
15. Azouaou N, Sadaoui Z, Djaafri A, Mokaddem H. Adsorption of cadmium from aqueous solution onto untreated coffee grounds: equilibrium, kinetics and thermodynamics. J Hazard Mater. 2010;184:126–34.
16. Zhu NY, Yan TM, Qiao J, Cao HL. Adsorption of arsenic, phosphorus and chromium by bismuth impregnated biochar: adsorption mechanism and depleted adsorbent utilization. Chemosphere. 2016;164:32–40.
17. Guo LQ, Ye PR, Wang J, Fu FF, Wu ZJ. Three-dimensional Fe_3O_4-graphene macroscopic composites for arsenic and arsenate removal. J Hazard Mater. 2015;298:28–35.
18. Mishra AK, Ramaprabhu S. Functionalized graphene sheets for arsenic removal and desalination of sea water. Desalination. 2011;282:39–45.
19. Wu LK, Wu H, Zhang HB, Cao HZ, Hou GY, Tang YP, et al. Graphene oxide/$CuFe_2O_4$ foam as an efficient absorbent for arsenic removal from water. Chem Eng J. 2018;334:1808–19.
20. Lin Q, Xu SH. A review on competitive adsorption of heavy metals in soils. Soils. 2008;40:706–11 [in Chinese].
21. Chen OP, Lin YJ, Cao WZ, Chang CT. Arsenic removal with phosphorene and adsorption in solution. Mater Lett. 2017;190:280–2.

22. Grafe M, Eick MJ, Grossl PR, Saunders AM. Adsorption of arsenate and arsenite on ferrihydrite in the presence and absence of dissolved organic carbon. J Environ Qual. 2002;31:1115–23.
23. Nabi D, Aslam I, Qazi IA. Evaluation of the adsorption potential of titanium dioxide nanoparticles for arsenic removal. J Environ Sci-China. 2009;21:402–8.
24. Zhang F. The efficiency and mechanism of cd/as immobilization by biochar and Iron-impregnated biochar [Master's thesis]. Changsha: Hunan Normal Univ; 2016 [in Chinese].